Proceedings of the ASME 2015 International Design Engineering Technical Conferences & Computers and Information in Engineering Conference
IDETC/CIE 2015
August 2-5, 2015, Boston, USA

DETC2015-46178

EXPERIMENTAL STUDY ON SINGLE WHEEL HUB MOTOR FAILURES AND THEIR IMPACT ON THE DRIVER-VEHICLE BEHAVIOR

Daniel Wanner*[1], Isabel Neumann[2], Lars Drugge[1], Peter Cocron[2], Maxim Bierbach[3] and Annika Stensson Trigell[1]

[1]Department of Aeronautical and Vehicle Engineering, KTH Royal Institute of Technology, Stockholm, Sweden

[2]Technische Universität Chemnitz, Department of Psychology, Chemnitz, Germany

[3]Active Vehicle Safety, Emissions and Energy, Federal Highway Research Institute (BASt), Bergisch Gladbach, Germany

ABSTRACT

An experimental field study investigating the impact of single wheel hub motor failures on the dynamic behavior of a vehicle and the corresponding driver reaction is presented in this work. The experiment is performed at urban speeds on a closed off test track. The single wheel hub motor failure is emulated with an auxiliary brake system in a modified electric vehicle. Driver reaction times are derived from the measured data and discussed in their experimental context. The failure is rated and evaluated objectively based on the dynamic behavior of the vehicle. Findings indicate that driver reactions are more apparent for the accelerator pedal compared to the steering wheel response. The controllability evaluation of the vehicle behavior shows that no critical traffic situation occurs for the tested failure conditions. However, even small deviations of the vehicle can impair traffic safety, specifically for other traffic participants like bicyclist and pedestrians.

NOMENCLATURE

C_i	Controllability class.
CI	Curve inner failure condition.
CO	Curve outer failure condition.
F	F-ratio.
M	Mean value.
N	Sample size.
Q_f	Fault influence index.
Q_x	Collision avoidance index.
Q_y	Lane keeping index.
Q_z	Vehicle stability index.
$Q^*_{x,y,z}$	Index classification.
S	Straight line driving failure condition.
SD	Standard deviation.
df	Degree of freedom.
p	Significance.
p_f	Brake pressure of auxiliary brake system.
t_δ	Steering wheel reaction time.
t_ε	Accelerator pedal reaction time.
δ	Steering wheel angle.
ε	Accelerator pedal position.
η_p^2	Effect size.
v_x	Longitudinal speed.
$\dot{\psi}$	Yaw rate.
a_x	Longitudinal acceleration.
a_y	Lateral acceleration.
$\dot{\psi}_m$	Mean yaw rate.
$\ddot{\psi}_{f,m}$	Mean yaw acceleration.
$\ddot{\Psi}$	Combined yaw rate difference and mean yaw acceleration.
ρ	Road curvature.

*Corresponding author. Email: dwanner@kth.se.

INTRODUCTION

Electric vehicles (EV) can be propelled by various types of drivelines. One promising type are drivelines incorporating wheel hub motors (WHM), which have several advantages like high efficiency or improved control of wheel torques [1]. In order to employ this propulsion concept in large scale, the risk of failure and possible failure modes should be analyzed. Currently, implications in case of a WHM failure during normal driving are not completely understood. Particularly, failures that will cause a braking torque to one of the wheels might be critical for driving safety and vehicle directional stability as it acts directly on the wheel. Recently, several studies have approached this specific research topic focusing on control strategies during a failure. A common WHM failure condition, i.e. an inverter shutdown, was investigated by Jonasson and Wallmark [2]. The failure was compensated by the means of an optimal control allocation strategy. Chu et al. [3] analyzed a similar fault accommodation strategy by implementing a failure that braked the right front wheel in an experimental vehicle. Results of both studies show the necessity and the potential of such control systems.

However, only little focus is put on the analysis of such a failure event, if neither a control allocation system nor a fault detection and diagnosis system to identify a failure are incorporated in the vehicle. Exceeding physical constraints and misinterpretation of control and diagnosis signals is further barely considered in the research field. Euchler et al. [4] studied three simple failure modes in an EV. The authors analyzed a positive, a negative and no propulsion torque on the WHM for three different friction levels. It was concluded that critical situations occur mainly during low friction levels or high lateral accelerations. Another study on various electrical and mechanical failures influencing the vehicle dynamic behavior has been conducted in [5]. Results show that the effect of a failure increases with higher vehicle speeds. However, low velocities should not be discarded as the failure depends heavily on the driveline and WHM design.

The main goal of this work is to analyze the influence of a specific WHM failure mode for urban speeds on the vehicle dynamic behavior and the response of the driver. A previously presented method for deriving driver reaction times [6] is described and applied. Further, it is analyzed how the failure is objectively rated according to the method developed by Wanner et al. [5] that is based upon the controllability classes of ISO 26262 [7].

The outline of the paper is as follows. First, the methodology of this work including the failure conditions, the experimental design, the modified EV and the test track as well as the sample are described. This is followed by the results section, analyzing the drivers' steering wheel and accelerator pedal reactions as well as the driver-vehicle behavior for each of the specified failure conditions.

METHODOLOGY

This experimental field study was a part of the European project EVERSAFE and analyses different failure conditions during normal operation of an electric passenger car. Data acquisition was conducted by Technische Universität Chemnitz (TUC) in cooperation with the Federal Highway Research Institute (BASt) [8]. Definition of failures and analysis of driver-vehicle response as well as the fault-classification was made by KTH Vehicle Dynamics in cooperation with TUC and BASt. The chosen failure conditions are defined for different driving maneuvers and are based on a typical failure mode in one of the WHM. The driving maneuvers were split into cornering and straight line driving, and conducted at urban speeds due to safety considerations during the experiment. The evaluation of the results is divided into a driver reaction analysis and an evaluation of the driver-vehicle behavior.

Failure conditions

Different failure conditions were specified before their implementation. The objective was to define each failure condition to affect the drivability of the vehicle, and thus having a distinct influence on the vehicle stability during normal driving. Each failure condition consisted of a certain driving maneuver and a corresponding failure mode. The selection of failure conditions was based on a broad study analyzing the effect of various failure modes and driving maneuvers on the dynamics of an electric vehicle [5].

Three driving maneuvers were chosen, a straight line driving maneuver with a failure on the left rear wheel (S), a left-hand cornering maneuver with a failure on the left rear wheel (curve inner (CI)) and a left-hand cornering maneuver with a failure on the right rear wheel (curve outer (CO)). Typical failure modes in an electric driveline that can be severe during vehicle speeds were investigated according to their influence on the dynamic behavior of a vehicle and integrated into the experimental set-up. The implemented failure mode represented a three-phase balanced short circuit in the WHM, which can for instance occur due to bad isolation of the windings inside the connection box or inside the active parts of the wheel hub motor [5, 9]. Three failure conditions were designed based on the urban speed of $30\,\mathrm{km/h}$ and the curvature was designed to achieve a lateral acceleration of $2-4\,\mathrm{m/s^2}$, i.e. for regular driving conditions [10].

Experimental design

The chosen experimental design was a within-subject design, which was applied as 3 (*failure condition*) x 2 (*anticipation*) design [8]. The effect of *failure condition* and *anticipation* on the controllability of the vehicle and the driver was tested. The within-subject factor *failure condition* was analyzed in the three mentioned maneuvers S, CI and CO. The second within-subject factor *anticipation* distinguished between unexpected and ex-

pected participants, which was covered by two different blocks; see Tab. 1. As safety precautions were taken during this field study and due to ethical reasons, the participants were informed that an event would occur that might deteriorate the driving behavior in the EV before the first block. Thus, the first failure occurred not completely unexpected for the drivers. The participants received information about the occurrence of another failure before the second block started, and thus, those failures were expected. Carryover effects in the within-subject design were compensated by arranging the test subjects randomly in three groups of failure condition sequences, as seen in Tab. 1. Thus, the very first failure occurrence for each of the three failure conditions could be analyzed.

Modified electric vehicle and test track

The chosen test vehicle was a Mitsubishi i-MiEV; see Tab. 2. It was equipped with an auxiliary brake unit on the rear axle that could be activated for each of the rear wheels independently, thus, simulating a single WHM failure according to the previously mentioned failure definition. The auxiliary brake unit was triggered from outside the vehicle via a remote control. When the failure was triggered, the desired value of the auxiliary brake pressure increased from 3 bar (idle) to 80 bar (maximum) on the selected rear wheel. The pressure developed in a ramp-shaped manner to 60 bar within 0.3 s, and converged slowly towards 80 bar afterwards. After 4.3 s, the desired brake pressure on the affected wheel returned to the idle pressure of 3 bar. The pressure build-up in the auxiliary brake unit is shown in Fig. 1. Further, the test vehicle was instrumented with a data acquisition system to record vehicle parameters such as speeds, directional and rotational accelerations during the experiment.

A closed-off parking lot in Chemnitz, Germany, was used to conduct the experiments. Fig. 2 shows the location of the failure conditions S, CI and CO on the test track. The field study was supposed to imitate an inner-city scenario with typical urban speeds of $30-50\,\mathrm{km/h}$. The subjects were instructed to maintain a driving speed of $30\,\mathrm{km/h}$ at which the failure happened as well. The course was only driven in counter-clockwise direction. A factor that conditioned the test track design was the desired lateral acceleration of $2-4\,\mathrm{m/s^2}$ during normal driving in urban environments [5]. Thus, the radius of both failure curves were set to 22 m.

TABLE 1. FAILURE CONDITION SEQUENCES.

Group name	First block			Second block		
FS 1	S	CO	CI	CI	CO	S
FS 2	CO	CI	S	S	CI	CO
FS 3	CI	S	CO	CO	S	CI

TABLE 2. TECHNICAL SPECIFICATION OF THE MODIFIED MITSUBISHI I-MIEV.

Parameter	Value
Curb weight	1192 kg
Wheel base	2550 mm
Center of gravity to front axle distance	1173 mm
Track width, front	1310 mm
Track width, rear	1270 mm
Drive system	RWD
Motor type	PMSM
Maximum power	49 kW
Maximum torque	180 Nm
Tyre dimensions, front	145/65 R15
Tyre dimensions, rear	175/55 R15

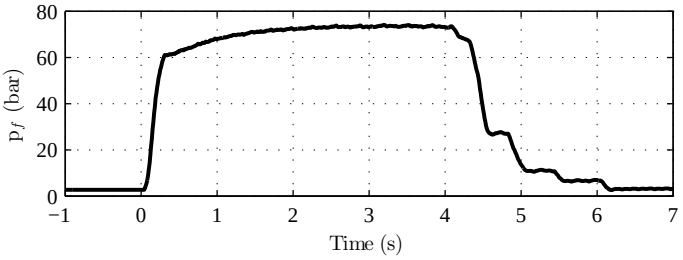

FIGURE 1. Pressure characteristics of auxiliary brake unit with failure activation at $t = 0\,\mathrm{s}$.

Sample

All participants were residents of the Chemnitz area in Germany and selected by public advertisements [8]. The sample size for the field study was $N = 49$ participants (37 men and 12 women), with an average age of $M = 31.4$ years ($SD = 5.7$) and ranging from $25-46$ years. The average annual mileage of the test subjects was 16980 km ($SD = 10820$). In average, they possessed their driver's license for $M = 12.3$ years ($SD = 5.7$ and range $2-28$ years). Almost half of the participants (40.8 %) had prior experience with either a hybrid-electric vehicle or an EV.

Procedure

At the beginning, consent was obtained and each participant was informed about the purpose of the experiment, the EV and the WHM. A familiarization period followed to get the participants comfortable on driving the course, following the target speed and putting them in a real-road driving context. Afterwards, one training round with the target speed was conducted in order to get a baseline measurement without failure interference.

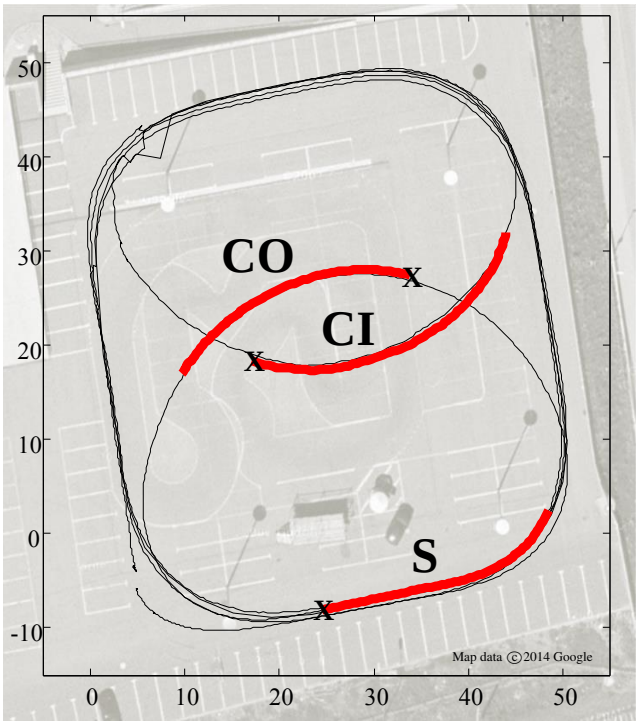

FIGURE 2. Illustration of the driven tracks in the experimental field study. Failure activation is indicated by markers (x) and red lines.

One round consisted of five laps on the test track, where three laps were driven on the outer edge and each curve was driven in one extra lap. The order was all-around, curve outward, all-around, curve inward and all-around [8]. At the end of the training, instructions on the task were given to complete the same round six times. In each round, a failure was triggered. Between each round, the participants had to stop and evaluate the round by filling in a questionnaire, which was identical every round. After the final questionnaire, each participant was provided with information about the project and the goals of this field study.

RESULTS

The findings of the experimental study are presented in this section, divided in an analysis of driver reaction and an analysis of driver-vehicle behavior. The results are focusing on the very first occurrence of a failure for each participant.

Driver reaction analysis

One of the most critical aspects of a failure condition in a vehicle is the reaction of the driver. Depending on the wheel on which the failure occurs, the driver feels that the vehicle is deviating from its intended path, driving either into the opposing lane or out of the road. An appropriate driver reaction should be counteracting the failure effect for an effective compensation. The quicker a driver counteracts to such a failure, the lower is the risk of an emerging dangerous situation.

The reaction times for accelerator pedal and steering wheel response were analyzed separately and are shown in Figs. 3–5 and Tab. 3 for the very first failure of each experimental group. The brake pedal was not used by most of the subjects due to the retardation caused by the failure, and thus it was not considered in the reaction time analysis. For each of the experimental groups, the mean values and 95 % confidence intervals of the steering wheel responses and accelerator pedal positions (in percent of the full pedal deflection) were calculated. These can be seen for the baseline without failure activation and the failure condition as seen in Figs. 3–5,(a) and (b). In addition, the mentioned mean values of baseline and failure condition were derived and the resulting rates were calculated for the steering rate difference according to

$$\Delta\dot{\delta} = \frac{\overline{\delta}_{Failure}}{dt} - \frac{\overline{\delta}_{Baseline}}{dt} \tag{1}$$

The accelerator pedal rate difference is determined accordingly. Both rate differences can be seen in Figs. 3–5,(c) and (d). A larger difference implied a larger offset on how fast steering wheel and accelerator pedal were utilized. In order to be counted as driver reaction triggered by the failure, the rate difference had to exceed a certain threshold that was defined by minimum and maximum rate difference. This threshold was determined during the two seconds prior failure activation and is marked by grey lines in Figs. 3–5,(c) and (d). As soon as the rate difference exceeded the threshold limits after failure activation, it was counted as initial reaction interval. The end of the initial reaction interval is found at the subsequent turning point of the rate difference curve. The reaction interval is marked by a bold black line. The mean reaction time of each parameter was then defined as the inflection point of the rate difference in the specified reaction interval. This method was used to define driver reaction times of the steering wheel (t_δ) and accelerator pedal (t_ε) for the three failure conditions.

The derived driver reaction times for failure condition S are displayed in Fig. 3. The steering wheel angle during the failure did not cross the thresholds for the first 1.5 s after failure activation. After this point in time, the steering wheel response due to the failure overlapped with the curve entrance of the test track, and thus might not have been related to the failure only, but also to the driver adapting to the change in road geometry. Hence, the steering wheel reaction time could not be determined. An individual analysis of steering wheel angle revealed that minor corrections $< 10^\circ$ were performed by several subjects 0.55 s after failure activation. Further, it could be seen in the baseline that the subjects were still steering back towards straight driving at

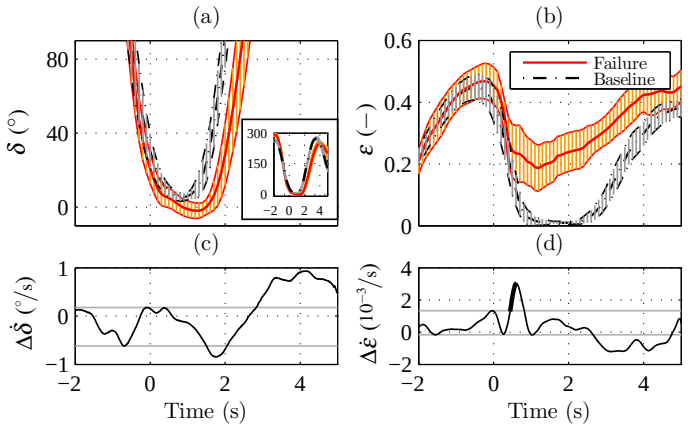

FIGURE 3. Confidence intervals of steering wheel angle (a) and accelerator pedal position (b) for baseline and failure condition of S with failure activation at $t = 0\,\mathrm{s}$. Corresponding rate difference of steering wheel angle (c) and accelerator pedal position (d).

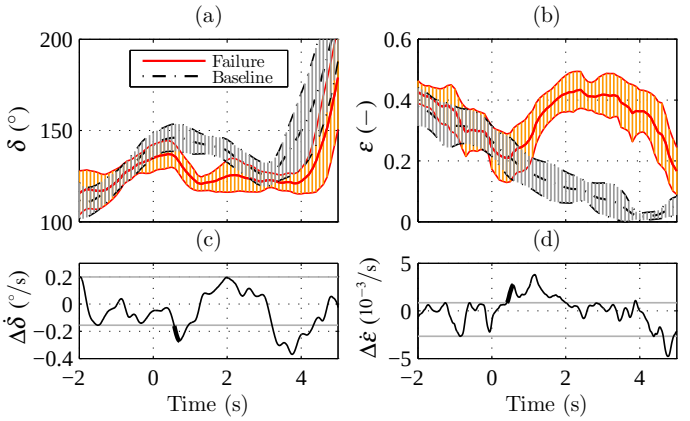

FIGURE 4. Confidence intervals of steering wheel angle (a) and accelerator pedal position (b) for baseline and failure condition of CI with failure activation at $t = 0\,\mathrm{s}$. Corresponding rate difference of steering wheel angle (c) and accelerator pedal position (d).

the point of failure activation. The accelerator pedal position (0-100 %) clearly showed a higher mean value of around 0.2 during an active failure. The reaction time was found to be 0.46 s with its reaction interval of $0.44\,\mathrm{s} < t_\varepsilon < 0.61\,\mathrm{s}$.

The reaction times for the failure condition CI are displayed in Fig. 4. The steering wheel angle during the failure dropped shortly after failure activation compared to the baseline. Its reaction time was found to be $t_\delta = 0.62\,\mathrm{s}$ with a reaction interval of $0.57\,\mathrm{s} < t_\varepsilon < 0.72\,\mathrm{s}$. The accelerator pedal was applied after $t_\varepsilon = 0.5\,\mathrm{s}$ (reaction interval: $0.41\,\mathrm{s} < t_\varepsilon < 0.58\,\mathrm{s}$).

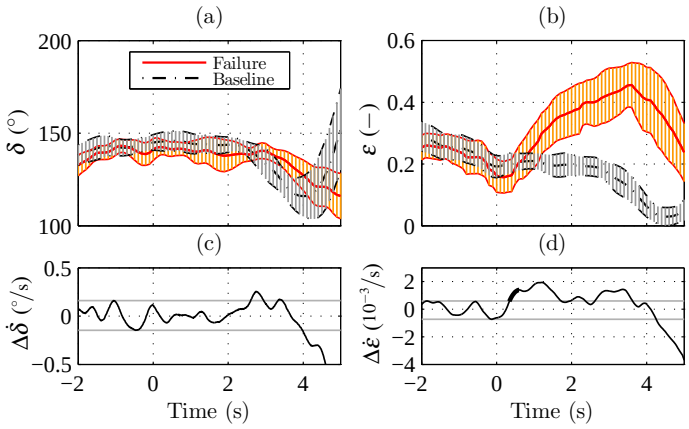

FIGURE 5. Confidence intervals of steering wheel angle (a) and accelerator pedal position (b) for baseline and failure condition of CO with failure activation at $t = 0\,\mathrm{s}$. Corresponding rate difference of steering wheel angle (c) and accelerator pedal position (d).

TABLE 3. DRIVER REACTION TIMES OF ACCELERATOR PEDAL AND STEERING WHEEL FOR THE ANALYZED FAILURE CONDITIONS.

Failure condition	t_δ (s)			t_ε (s)		
	Min	Mean	Max	Min	Mean	Max
S	-	-	-	0.44	0.46	0.61
CI	0.57 s	0.62	0.72	0.41	0.50	0.58
CO	-	-	-	0.34	0.40	0.60

The steering wheel reaction time of CO was not determinable from the results, see Fig. 5. The difference in steering wheel angle around 2.76 s was based on the upcoming curve and the fact that the vehicle was at a different position on the test track due to the speed difference of failure and baseline run, and thus it was not counted as steering wheel reaction time. The accelerator pedal reaction time showed a clear trend of applying the pedal after 0.4 s with its reaction interval of $0.34\,\mathrm{s} < t_\varepsilon < 0.60\,\mathrm{s}$.

The main effects of the steering wheel and accelerator pedal signals have been analyzed in repeated measures analyses of covariance (RMANCOVA) [11] as seen in Tab. 4. The within-subject factors were time and failure state (baseline vs. failure), while the co-variate was the difference of the respective parameters between the failure states for both input signals at the time of failure activation. The tested period started with the previously derived reaction time until three seconds after failure activation. Note that results are only reported for the factor failure state. The main effect of the failure state for the accelerator pedal re-

TABLE 4. RMANCOVA RESULTS OF STEERING WHEEL AND ACCELERATOR PEDAL SIGNALS FOR THE FIELD STUDY (COVARIATE: $\Delta\delta(T_0)$ AND $\Delta\varepsilon(T_0)$).

Results of steering wheel reaction				
Failure condition	df	F	p	η_p^2
S	-	-	-	-
CI	13	125.3	$< .001$	.906
CO	-	-	-	-
Results of accelerator pedal reaction				
Failure condition	df	F	p	η_p^2
S	16	16.28	$< .001$	.504
CI	13	97.79	$< .001$	.883
CO	15	22.89	$< .001$	.604

actions were statistically significant for each of the three failure conditions. This underlines the findings of the accelerator pedal reaction time analysis as seen in Figs. 3–5,(b). The plots clearly show that the participants pushed the accelerator pedal after the failure occurred in order to compensate for the speed decrease caused by the failure for all failure conditions. The statistical analysis of the steering wheel angle was only conducted for CI as t_δ could not be determined for S and CO. Failure condition CI showed also a clear significance for the main effect failure state. In Fig. 4(a), the counter-steering of the participants is clearly visible at $0.5 - 2.5$ s.

Driver-vehicle behaviour

The results for the driver-vehicle behavior are shown in Figs. 6–8. The baseline for each failure condition was calculated from the measured data of the baseline run and the first part of the first failure run up to the first failure activation. The characteristics of the corresponding baseline parameters were averaged for each experimental group at the stretches of the three failure conditions. Previously defined reaction times and the failure activation are marked with black dashed and solid lines.

The driver-vehicle response of failure condition S is depicted in Fig. 6. Due to size limitations of the test track, the straight line driving maneuver was not at steady-state condition at the point of failure activation and had to be seen in perspective to its constraints. The failure was activated at the exit of a curve where most of the subjects were accelerating in order to reach the target speed of 30 km/h in the subsequent straight section. Further on, the straight stretch of the failure activation was just $10 - 15$ m long. Thus, most participants drove in two rather large clothoids without a straight section in between, instead of driving completely straight. Depending on the driving strategy of each driver, this distance was traveled in $1.2 - 1.8$ s at 30 km/h. Together with

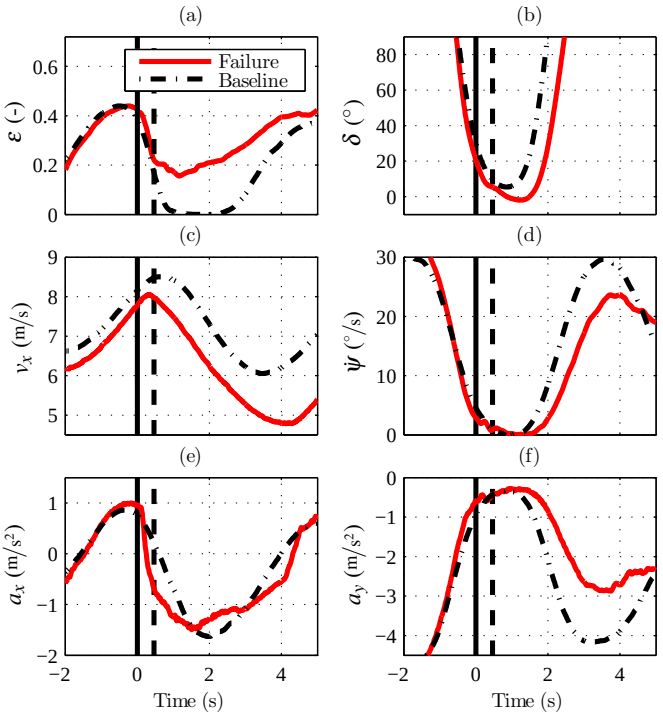

FIGURE 6. Driver-vehicle responses of baseline and failure condition S, including failure activation at $t = 0$ s (black vertical line) and reaction time at $t_\varepsilon = 0.46$ s (black dashed line).

the occurring deceleration triggered by the failure, it explained the offset between baseline and failure parameters beyond 1.5 s.

The influence of the failure on the vehicle speed (Fig. 6(c)) was visible after 0.4 s. Due to the increase of accelerator pedal position after $t_\varepsilon = 0.46$ s (Fig. 6(a)), the speed difference during the rest of the failure stretch was about 2 km/h (0.56 m/s), considering the existing offset before failure activation. Even though the longitudinal acceleration of the baseline was changing (Fig. 6(e)), the impact of the failure was clearly seen with -1 m/s² after 0.3 s. However, except for the deceleration of the vehicle, only negligible changes could be observed in yaw rate and lateral acceleration before the first driver reaction (Figs. 6(d) and (f)).

The vehicle states during failure condition CI are shown in Fig. 7. The failure generates an instant longitudinal acceleration of -1.1 m/s², see Fig. 7(e). The subsequent change in accelerator pedal position intercepted its further decrease. The longitudinal acceleration was fully compensated for after 2 s. The change in vehicle speed became more apparent for CI with 5 km/h (1.4 m/s) difference after 2 s (Fig. 7(c)). The lateral acceleration was initially increasing (Fig. 7(d)). As the driver reaction time was reached, it strongly decreased as the steering wheel angle started to compensate for it, as it is shown in Fig. 7(b). The yaw

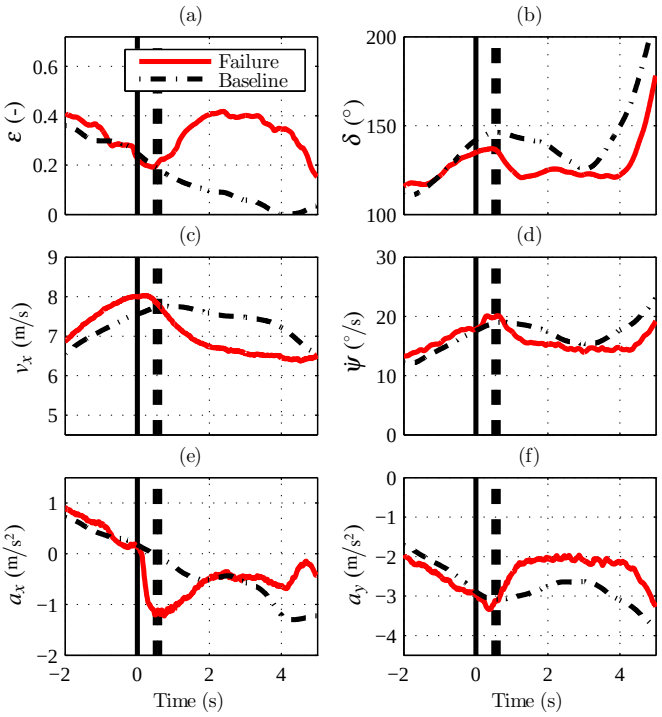

FIGURE 7. Driver-vehicle responses of baseline and failure condition CI, including failure activation at $t = 0\,\mathrm{s}$ (black vertical line) and reaction times at $t_\delta = 0.62\,\mathrm{s}$ and $t_\varepsilon = 0.5\,\mathrm{s}$ (black dashed lines).

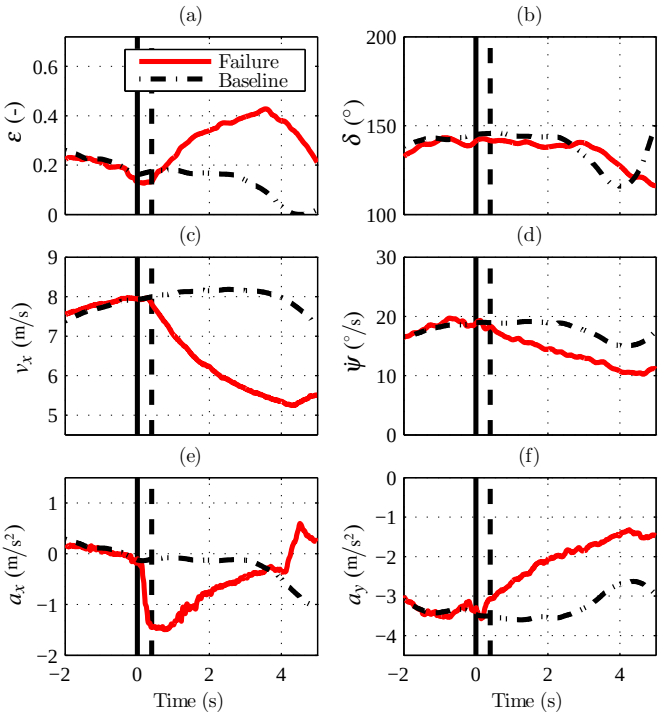

FIGURE 8. Driver-vehicle responses of baseline and failure condition CO, including failure activation at $t = 0\,\mathrm{s}$ (black vertical line) and reaction time at $t_\varepsilon = 0.4\,\mathrm{s}$ (black dashed line).

motion showed an incline before the first driver reaction. After the driver reaction, the yaw rate decreased further under the level of the baseline run due to the change in steering wheel angle.

In Fig. 8, failure condition CO showed the highest influence on longitudinal acceleration ($-1.5\,\mathrm{m/s^2}$) and vehicle speed decrease ($10\,\mathrm{km/h}$ ($2.8\,\mathrm{m/s}$) after 4 s) as shown in Figs. 8(c) and (e). One clarification could be the constant longitudinal acceleration of the baseline for this failure stretch compared to S and CI. In other words, the subjects kept the longitudinal acceleration constant during the baseline run, which increased the difference between baseline and failure condition. The yaw rate was reduced, while the lateral acceleration rose from $-3.5\,\mathrm{m/s^2}$ to $-1.5\,\mathrm{m/s^2}$ directly after failure activation (Figs. 8(d) and (f)). However, it was a slight change, which was compensated not mainly by the driver, but due to the reduced under-steering behavior of the experimental vehicle with speed decrease.

The main effects of the failure state (baseline and failure) were also calculated with RMANCOVAs for yaw rate and lateral acceleration. The statistical results supported the findings above as seen in Tab. 5. Except for the main effect of the failure state for the yaw rate during CI, none of the other main effects had a statistical significance.

The driver-vehicle behavior for each failure condition was further evaluated with respect to its controllability class according to ISO 26262. A fault classification method [5] was applied to classify each failure condition. Hereby, the potential risk of longitudinal, lateral and yaw motion were separately evaluated by three indexes first. The collision avoidance index Q_x is defined as the sum of the longitudinal speed and acceleration difference in a certain time period. The lane keeping index Q_y is defined as the point in time when the first wheel of the vehicle leaves the lane. Here, the test subject never left the lane, and thus Q_y was not considered. The vehicle stability index Q_z is defined as the sum of the yaw rate difference $\Delta\dot{\psi}_m$ and the mean yaw acceleration $\ddot{\psi}_{f,m}$ in a certain time period

$$\ddot{\Psi} = \frac{\Delta\dot{\psi}_m}{t_\delta} + \ddot{\psi}_{f,m}, \tag{2}$$

and depends on the vehicle states in case of a cornering maneuver according to

$$Q_z = \mid \ddot{\Psi} \mid + 0.5(\mathrm{sign}(\ddot{\Psi})\mathrm{sign}(\delta) - 1)v_x \rho s^{-1}. \tag{3}$$

This enables a distinct evaluation of the vehicle directional stability depending on its over-/ under-steering behavior induced by

TABLE 5. RMANCOVA RESULTS OF YAW RATE AND LATERAL ACCELERATION FOR THE FIELD STUDY (CO-VARIATE: $\Delta\psi(T_0)$ AND $\Delta A_Y(T_0)$). NOTE THAT RESULTS ARE ONLY REPORTED FOR THE FACTOR FAILURE CONDITION.

Results of yaw rate				
Failure condition	df	F	p	η_p^2
S	16	2.751	.117	.147
CI	13	8.916	.011	.407
CO	15	1.709	.211	.102
Results of lateral acceleration				
Failure condition	df	F	p	η_p^2
S	16	2.784	.115	.148
CI	13	1.831	.199	.123
CO	15	.039	.845	.003

TABLE 6. CONTROLLABILITY CLASS DEFINITION OF THE THREE INDEXES.

Controllability classes	C_0	C_1	C_2	C_3
$\mid Q_x \mid$ in $^{\mathrm{m}}/_{\mathrm{s}^2}$	< 0.8	$0.8-2.3$	$2.3-3.0$	> 3
$\mid Q_y \mid$ in s	> 5	$5.0-3.0$	$3.0-2.0$	< 2
Q_z in $^{\circ}/_{\mathrm{s}^2}$	< 2	$2.0-3.5$	$3.5-5.0$	> 5
$Q^*_{x,y,z}$	1	2	3	9
Q_f	3	4	$5-8$	$>= 9$

the failure and the location of the failure. The time period in this study was defined based on the accelerator pedal and steering wheel reaction times; i.e. $0.5\,\mathrm{s} \pm 0.25\,\mathrm{s}$ for Q_x and $0.6\,\mathrm{s} \pm 0.25\,\mathrm{s}$ for Q_z. Secondly, a fault influence index merges these three partial indexes to a final rating of controllability of the three analyzed failure conditions. In Tab. 6, the definitions of the three indexes and the controllability classes reaching from C_0 (easy to control) to C_3 (uncontrollable) are shown.

The calculated controllability classes of the driver-vehicle behavior for each failure condition are shown in Tab. 7. All failure conditions were rated with the controllability class C_1. With other words, none of the failure conditions was safety critical. Note that the measured data from the GPS-signal had a too low resolution in order to analyze lateral deviation and derive the lane keeping index.

TABLE 7. CONTROLLABILITY CLASSIFICATION FOR THE THREE FAILURE CONDITIONS IN THE FIELD STUDY.

Failure condition	Q_x ($^{\mathrm{m}}/_{\mathrm{s}^2}$)	Q_y (s)	Q_z ($^{\circ}/_{\mathrm{s}^2}$)	Q_f (-)	Controllability class
S	1.65	–	1.40	4	C_1
CI	1.10	–	1.36	4	C_1
CO	1.83	–	−13.05	4	C_1

DISCUSSION

This work presented a study of driver reactions and driver-vehicle behavior to three different WHM failure conditions. The proposed method of deriving driver reaction times was found to be suitable. Reaction times from several crosswind and brake reaction studies [12, 13, 14] are in the same range as the reaction times that were found with this approach. The reported findings showed that the effects of the tested failure mode at $30\,^{\mathrm{km}}/_{\mathrm{h}}$ during straight lane driving and cornering could be handled by drivers and were not critical to the driving safety of the vehicle for the driven maneuvers.

The main driver reaction for all failure conditions in this field study was the increased accelerator pedal position with short reaction times of $t_\varepsilon = 0.4-0.5\,\mathrm{s}$ (Tab. 3), and thus overruling the deceleration due to the failure. A significant steering wheel reaction could be found for the curve inward failure. The instructions of the participants to keep a speed of $30\,^{\mathrm{km}}/_{\mathrm{h}}$ could be an explanation for this result. Another reason could be this relatively low speed during an active failure, which was accompanied by a smaller lateral offset. Thus, the drivers might not react as distinctively to a failure condition at low speeds compared to one at higher speeds. Similar experiments in a driving simulator show that lateral course deviations caused by a single WHM failure are significantly higher for motorway speeds [8]. Further, the longitudinal deceleration triggered by the failure felt considerably stronger compared to the effect the failure had on the lateral motion of the modified EV.

This study is constraint by excluding the influence of other road traffic and different road conditions (e.g. rain and ice). As an additional limitation, it must be considered that all subjects were informed that a failure could occur, and therefore the reaction times may not be comparable to reaction times when the failure would occur in real traffic for the first time. Thus, other conditions might lead to critical driving situations. In order to analyze this further, the same failure conditions were simulated due to the low precision quality of the measured GPS-signal. Results when applying the derived reaction times show that the simulated vehicle left its trajectory by up to 0.2 m in lateral direction for the exact same failure conditions, thus inherently stays within its lane. Slower steering wheel reaction times were simulated additionally ($t_\delta = 2.5\,\mathrm{s}$) and showed lateral deviations up

to 0.6 m. Based on the latter results, a critical situation for other traffic participants and vulnerable road users, such as bicyclists and pedestrians, could occur.

The objective evaluation showed that none of the analyzed failures is highly critical for driving safety as the controllability class C_1 is reached for all failure conditions. Another maneuver in the simulation environment was studied in order to analyze one of the most severe failures that could happen with an WHM, i.e. locking the inner rear wheel. It was shown that the vehicle would leave its lane after 1.5 s, stopping at a maximum achievable lateral deviation of 1.8 m.

The subjective evaluation has been conducted in [8]. Its findings showed that most participants (94 %) realized the failure while driving. Perceived risk and stress as well as lack of control during the failure were not significantly higher than during the baseline for the failure conditions CI and CO. Thus, no significant effects were found for a failure while cornering, which was an unexpected result. The straight line failure condition S showed significant effects for all three evaluation parameters on the other hand. A viable explanation could be that the perception of a failure is different for curves and straight road sections. Yaw rate and lateral acceleration suddenly appear for a failure during straight line driving, while both parameters are already present during cornering, and then only change to other amplitudes. Another reason could also be the relatively high ratings of the curve baseline condition in comparison to the relatively low ratings of the straight baseline condition [8]. Finally, the relatively low velocity of 30 km/h might also be accounted for these results, which is accompanied by the small vehicle dynamic effect of the failures as seen in Tab. 7.

CONCLUSIONS

The aim of this research work was to study driver-vehicle behavior caused by a WHM failure mode in an experimental field study. Three failure conditions have been analyzed for a vehicle speed of 30 km/h. The failure was implemented in a modified EV and the experiments were conducted on a closed test track. A method for defining driver reaction times has been presented and reaction times for steering wheel and accelerator pedal were analyzed. Objective results of each failure condition were evaluated according to a controllability classification method and finally compared to the subjective results.

This work has shown that typical failure modes in WHM can influence the driver-vehicle behavior only to a small extent in the studied speed. The steering wheel response was distinct for the curve inward failure only. For the accelerator pedal response, the opposite was valid. Drivers reacted faster on the accelerator pedal to the failure, which could be attributed to the instructions of the participants to keep their speed at all times. Different instructions could cause considerably different driver behaviour. The driver-vehicle behavior showed that none of the three analyzed failure conditions led to vehicle instabilities as the drivers could compensate for it. Nevertheless, these failures can lead to critical situations in traffic. The resulting speed reduction could lead to consequences for following traffic and different road conditions or traffic situations could lead to more critical situations as well. Further, due to such failure conditions, other traffic participants could be harmed.

The influence of traffic, different road conditions and an electronic stability control system was excluded, but could be analyzed in future studies. The data analysis could also be the basis for a driver model that is valid during a failure. In addition, control strategies such as control allocation could be integrated into the vehicle to handle such failures, and hence supporting the driver to maneuver the vehicle on its intended path.

Acknowledgements

This study is part of the EU Project EVERSAFE, which is funded by the ERA-Net Transport Electromobility+ Program. The support of all project partners is gratefully acknowledged. Special thanks goes to Patrick Seiniger from BASt, who supported the failure implementation and instrumentation of the modified EV and to the team at TUC for their contributions during planning and conducting the field study. Further financial support is gratefully acknowledged to the SHC Swedish Hybrid vehicle Center.

REFERENCES

[1] N. Borchardt, R. Kasper and R. Heinemann, *Design of a wheel-hub motor with air gap winding and simultaneous utilization of all magnetic poles*, Proc. of IEEE International Electric Vehicle Conference (IEVC), Greenville, United States, 2012.

[2] M. Jonasson and O. Wallmark, *Control of electric vehicles with autonomous corner modules: implementation aspects and fault handling*, Int. J. Vehicle Systems Modelling and Testing, vol. 3, no. 3, 2008, pp. 213–228.

[3] W. Chu, Y. Luo, Y. Dai, and K. Li, *Traction fault accommodation system for four wheel independently driven electric vehicle*, Proc. of 26th Electric Vehicle Symposium, Los Angeles, United States, 2012.

[4] M. Euchler, T. Bonitz, M. Geyer and D. Mitte, *Evaluation of the dynamic stability of an electric driven vehicle during safety-critical situations in steady state cornering*, VDI-Berichte, 2009, vol. 2086, pp. 316–333.

[5] D. Wanner, L. Drugge and A. Stensson Trigell, *Fault classification method for the driving safety of electrified vehicles*, Veh. Sys. Dyn., vol. 52, no. 5, 2014, pp. 704-732.

[6] D. Wanner, M. Kreußlein, B. Augusto, L. Drugge and A. Stensson Trigell, *Single wheel hub motor failures and*

their impact on vehicle and driver behaviour, submitted for publication in Oct. 2014.

[7] ISO 26262, *International standard of functional safety for road vehicles*, 1 – 10, 2011.

[8] P. Cocron, I. Neumann, M. Kreußlein, M. Pereira, D. Wanner, L. Drugge, M. Bierbach and B. Augusto, *Driver and vehicle behaviour to power train failures in electric vehicles experimental results of field and simulator studies*, technical report D2.1, EVERSAFE Electromobility+ Project, 2014.

[9] O. Wallmark, *Control of permanent-magnet synchronous machines in automotive applications*, Doctoral Thesis, Chalmers University of Technology, Sweden, 2007.

[10] Robert Bosch GmbH (ed.), *Kraftfahrtechnisches Taschenbuch*, Vieweg, 2007.

[11] A. Field, *Discovering statistics using SPSS*, SAGE Publications, 2009.

[12] M. Green, *How long does it take to stop? Methodological analysis of driver perception-brake times*, Transportation Human Factors, vol. 2, 2000, pp. 195.-216.

[13] W. W. Wierwille, J. G. Casali and B. S. Repa, *Driver steering reaction time to abrupt-onset crosswinds, as measured in a moving-base driving simulator*, Human Factors, vol. 25, no. 1, 1983, pp. 103–116.

[14] J. Jarlmark, *Driver-vehicle interaction under influence of crosswind gusts*, Licentiate Thesis in Vehicle Engineering, TRITA-FKT 2002:18, Royal Institute of Technology, Stockholm, Sweden, 2002.